Comments on Inorganic Chemistry
Publication details, including instructions for authors and subscription information:
http://www.informaworld.com/smpp/title~content=t713455155

Advances in High-Resolution Laser Spectroscopy of Coordination Compounds

Hans Riesen[a]; Elmars Krausz[a]
[a] Research School of Chemistry, The Australian National University, Canberra, Australia

To cite this Article Riesen, Hans and Krausz, Elmars(1993) 'Advances in High-Resolution Laser Spectroscopy of Coordination Compounds', Comments on Inorganic Chemistry, 14: 6, 323 — 347
To link to this Article: DOI: 10.1080/02603599308048667
URL: http://dx.doi.org/10.1080/02603599308048667

Advances in High-Resolution Laser Spectroscopy of Coordination Compounds

HANS RIESEN and ELMARS KRAUSZ
Research School of Chemistry,
The Australian National University,
Canberra, ACT 0200,
Australia

Received January 14, 1993

Advanced laser spectroscopies are shown to be invaluable in providing unambiguous detail concerning the electronic structure of coordination compounds. The basic principles of two techniques which overcome the effect of inhomogeneous broadening, namely fluorescence line narrowing and hole-burning spectroscopy, are discussed. Their use and limitations in transition-metal complexes along with examples from our own work are given. These examples present a full range of d-d, ligand-centered singlet–triplet and charge-transfer transitions in both crystalline and amorphous hosts.

Key Words: *fluorescence line narrowing, hole-burning, homogeneous linewidth, inhomogeneous broadening*

1. INTRODUCTION

The optical spectroscopy of insulating solids has experienced remarkable progress over the last two decades. This progress is mainly due to the advent of stable single-frequency dye lasers. Linewidths

Comments Inorg. Chem.
1993, Vol. 14, No. 6, pp. 323–347
Reprints available directly from the publisher
Photocopying permitted by license only

as low as Hz to kHz have been achieved for optical transitions in solids. (Note that 1 kHz corresponds to 3.3×10^{-8} cm^{-1}!). This kHz linewidth has to be compared to the few hundred THz of optical transitions, i.e., the resolution can be about one part in 10^{12}. This level of resolving power exceeds that available in any other technique.

Excellent reviews of the various laser spectroscopies have been published over the last decade.[1-6] A very good description of advanced instrumentation is found in the outstanding book by Demtröder.[7]

Most work has been devoted to the study of either rare earth doped oxides and halides or organic molecules embedded in various hosts. However, coordination compounds have received relatively little attention.

The present Comment outlines the basic principles of two laser spectroscopies, namely Fluorescene Line Narrowing (FLN) and spectral hole-burning, and of course special emphasis is put on applications to coordination compounds.

First, we discuss some basic aspects of the electronic spectroscopy in the solid state to gain some insight into the potential, but also the limitations of advanced laser spectroscopies.

1.1. The Homogeneous Linewidth

In an electronic system with two isolated levels (see Fig. 1) the lineshape of the electronic transition is Lorentzian. The full width at half maximum Γ_{hom} is determined by the pure dephasing time T_2^* and the lifetime T_1 of the excited state [Eq. (1)]. T_1 is given by the radiative, k_r, and non-radiative, k_{nr}, relaxation rates, $1/T_1 = k_r + k_{nr}$.

$$\Gamma_{hom} = 1/[(2\pi T_2)(1 + \omega_1^2 T_1 T_2)^{1/2}] \tag{1}$$

where

$$1/T_2 = 1/T_1 + 2/T_2^*. \tag{2}$$

T_2 in Eq. (2) is called the effective dephasing time. The pure dephasing time T_2^* is often dominated by the quasi-elastic scatter-

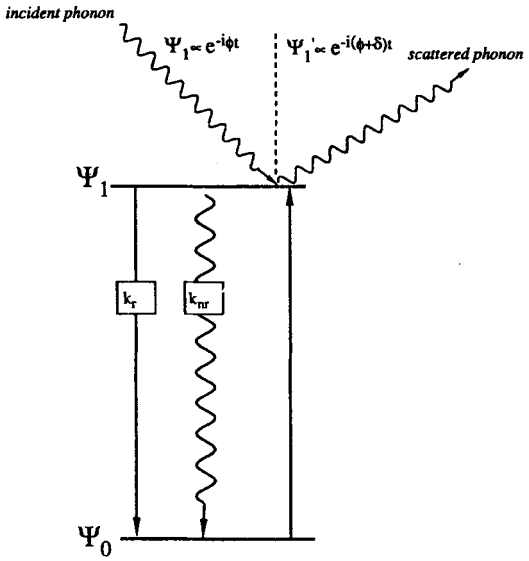

FIGURE 1 Transitions between two electronic levels Ψ_0 and Ψ_1. k_r and k_{nr} denote the radiative and nonradiative relaxation rates, respectively. The quasi-elastic scattering of a phonon is depicted schematically for the excited state.

ing of phonons. As is schematically shown in Fig. 1 the time-dependent part of the wavefunction Ψ_1 changes its phase ϕ by δ after the scattering process. The dephasing process also occurs in the ground state, which gives rise to a factor of two in Eq. (2). Electronic and nuclear spin fluctuations can contribute significantly to the dephasing process.

The Rabi frequency ω_1 is proportional to the *amplitude* of the incident light, and thus the power broadening term $\omega_1^2 T_1 T_2$ can be neglected if the laser power is kept low enough. In this case Eq. (1) simplifies to

$$\Gamma_{hom} = 1/2\pi T_2. \tag{3}$$

There are very few phonons excited at liquid helium temperatures, and the dephasing time T_2^* is usually long relative to the lifetime T_1 of the excited state. In this case Γ_{hom} is determined by T_1 only. In contrast, at room temperature the dephasing time can give large contributions to the linewidth ($\sim$10 cm^{-1}). Within the

Debye approximation for the density of phonon states, the quasi-elastic scattering of phonons is predicted to be proportional to T^7 at lowest temperatures.

1.2. Inhomogeneous Broadening

Equation (1) is only applicable to an ensemble of identical chromophores, i.e., a perfect crystal. However, all real solid state systems suffer from inhomogeneous broadening. The chromophoric units have slightly different environments (see Fig. 2). In crystals this is due to dislocations, strains, unintentional impurities, disorder and so forth. In amorphous hosts there is no long range order. Inhomogeneities are far more severe and a wide range of distortions of the chromophoric unit are possible. The width and shape of the distribution of purely electronic origins is determined by the effective local fields. Inhomogeneously broadened transitions are often found to be Gaussian but more complicated lineshapes have been observed in a number of crucial examples.

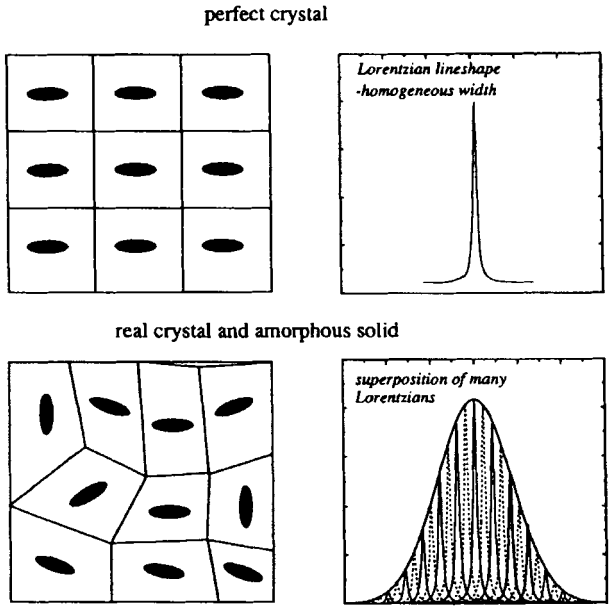

FIGURE 2 Schematic representation of the source of inhomogeneous broadening in the solid state.

One particular source of inhomogeneous broadening in coordination compounds is the variation of metal–ligand distances. We take the particular example of the $^4A_2 \leftrightarrow {}^4T_2$ ligand-field transition in d^3 systems, e.g., $[Cr(NH_3)_6]^{3+}$. The transition energy is given in a first order approximation by $10Dq$. From the definition of the octahedral ligand-field parameter Dq in Eq. (4) one can easily derive Eq. (5).

$$Dq = Ze^2\langle r^4\rangle_{3d}/6R^5, \tag{4}$$

$$\partial Dq/Dq = -5\partial R/R. \tag{5}$$

Z is the effective charge of the metal ion, $\langle r\rangle$ is the radial density function of the 3d electrons, and R is the metal–ligand separation.[8]

If we take $Dq = 2000\ cm^{-1}$ and $R = 2$ Å it follows that $\partial R/R = 0.001$, $\partial R = 0.002$ Å, and $\partial(10Dq) = -100\ cm^{-1}$. Thus minute changes in the metal–ligand separation R can lead to considerable shifts of electronic energies. Clearly, variations in the metal–ligand separation are a likely source for any lack of fine structure in spin-allowed ligand-field transitions in coordination compounds.

Transitions which occur within the same electronic configuration (e.g., t_2^3) are less vulnerable to inhomogeneous broadening because they are independent on the ligand-field strength in a first order approximation. For instance the $^4A_2 \leftrightarrow {}^2E$ spin-flip transition in chromium(III) systems is usually found to be (relatively) sharp.

1.3. Vibrational Sidebands

The visibility of a purely electronic origin depends on not only the inhomogeneous broadening but also on the Huang-Rhys[9] parameter S as is illustrated in Fig. 3 for the progression of one total symmetric mode based on the electronic origin. Spin-allowed d-d transitions between different electronic configurations show Huang–Rhys parameters of about 3 to 5, i.e., the potentials of the ground state and the excited state have a relatively large displacement. The vibrational sidebands are very pronounced in this case and the electronic origin carries only a fraction of the total intensity ($I_{origin}/I_{total} = e^{-S}$). The electronic origin is hardly recognizable

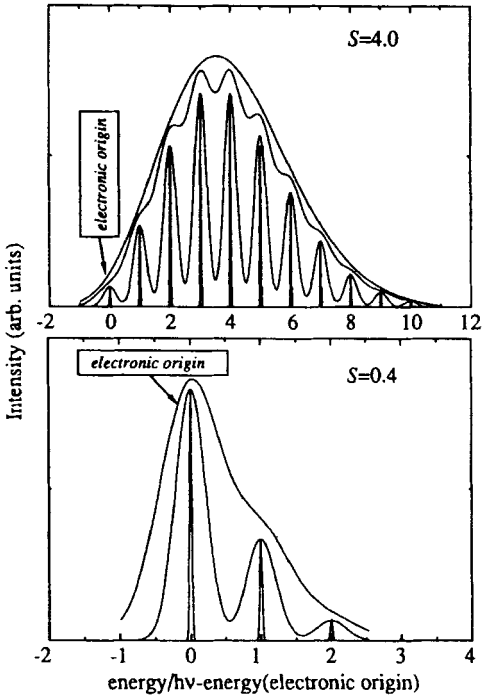

FIGURE 3 Inhomogeneous broadening and the lineshape of the vibrational sideband for two Huang–Rhys parameters S. $\Gamma_{inhom}/\hbar\omega$ = 0.04, 0.5, 1.0, 1.5 and 0.04, 0.5, 1.0 for the upper and lower spectra, respectively. A single progression of a total symmetric mode is assumed.

in a spectrum where the inhomogeneous width is comparable to the energy $\hbar\omega$ of a total symmetric breathing mode for $S = 4$.

In contrast, for transitions within the same electronic configuration, i.e., transitions with small values of S, the origin can always be observed because the vibronic sidebands carry only little intensity. In Fig. 3 we have assumed the same linewidth for the vibrational levels as for the electronic origins. This assumption becomes valid if the inhomogeneous width exceeds $1/2\pi T_1$ of the vibrational levels ($\sim$10 cm^{-1}). In the homogeneous spectrum, vibrational sidebands then have broader linewidths than the electronic origin at low temperature because of the fast relaxation processes (thermalization).

Only features which are recognizable in conventional spectroscopy can be readily narrowed by the laser spectroscopies discussed in this Comment.

1.4. The Correlation of Electronic Levels in the Solid State

In most cases the energies of electronic states are dependent on more than one parameter. This may lead to electronic levels being poorly correlated because there is a range of parameters which give the same energy difference between the initial and final level. For instance the energies of d-states are determined by the octahedral ligand field parameter Dq, the Racah parameters B and C which take into account the electronic repulsion, the spin-orbit coupling constant and parameters which describe the effect of lower fields (if present), e.g., trigonal or tetragonal field.

In amorphous hosts transition metal complexes will experience all possible distortions, and also the local electrostatic fields of the outer sphere will have a substantial spread. Thus the distribution of energy levels generally involves many parameters, and the correlation of energy levels may be very poor. Hence FLN and hole-burning are mainly energy selective and *not* site-selective techniques *in amorphous hosts*.[10,11]

The inhomogeneous widths are usually less in crystalline environments although homogeneous widths may in fact be greater than for the same chromophore in amorphous hosts, particularly for temperatures above 10 K. In general energy splittings vary by less than a few percent over inhomogeneous distributions in crystalline matrices reflecting a high correlation of energy levels. By contrast, the inhomogeneous broadening seems to be far less systematic in amorphous hosts.

1.5. Non-Radiative Relaxations

Usually only the lowest-excited state of coordination compounds is luminescent. This is because most compounds have high frequency vibrations which can act as energy acceptors to bridge the gap between higher-lying excited states and the lowest excited state. The probability of a *multiphonon* relaxation is a function of the number of vibrational quanta which have to be created.[12,13] Compounds with high energy frequencies (e.g., N–H, C–H and

O–H stretches) will not show any luminescence from higher-lying excited states because only few vibrational quanta have to be created. Also if the lowest excited state lies below 10,000 cm^{-1} the quantum efficiency for the luminescence may become very low. Fast multiphonon relaxation to the lowest excited state may substantially shorten the lifetime T_1 of higher-lying excited states and thus contribute to their homogeneous linewidths.

The energy gap between electronic levels often lies within the range of phonon energies (~0–3000 cm^{-1}). This situation makes the direct one–phonon relaxation possible. In a Debye approximation for the density of phonon states the rate k_0 of a direct process at $T = 0$ K (see Fig. 4) is expected to be proportional to the third power of the gap.[9] This reflects the vanishing density of phonon states at low energies, and the relaxation betwen very-close-lying states (<0.5 cm^{-1}) may become slow compared to the luminescence lifetime.

The temperature dependence of the direct process is given in Eqs. (6) and (7) for the emission k_e and absorption k_a of a phonon of energy $\hbar\omega$, respectively.

$$k_e = k_0(\bar{n} + 1), \tag{6}$$

$$k_a = k_0\bar{n}, \tag{7}$$

where

$$\bar{n} = 1/(\exp(\hbar\omega/kT) - 1). \tag{8}$$

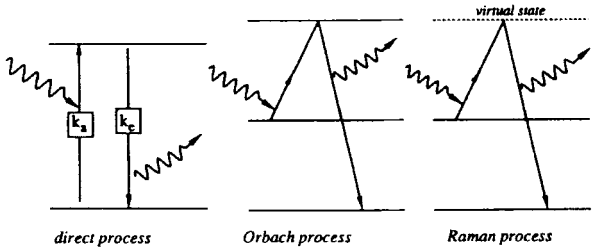

FIGURE 4 One- and two-phonon processes leading to relaxation between close-lying electronic states. The wavy arrow represents the phonons involved in the process.

It is clear that the direct process may give a substantial contribution to the homogeneous linewidth of higher-lying excited states in coordination compounds because of the large number of vibrational modes. Using Eq. (1) a homogeneous broadening of 1 cm^{-1} is predicted for a relaxation rate of 2×10^{11} s^{-1} ($T_1 = 5$ ps).

Orbach processes may also contribute to the non-radiative transitions between close-lying levels. As is illustrated in Fig. 4, an Orbach relaxation process involves two phonons and three electronic levels.

A third possible mechanism is the two phonon Raman process also illustrated in Fig. 4. This mechanism is related to the Orbach process but in this case the intermediate level is a virtual state.

If the splitting is about 50 cm^{-1} the direct process often determines the temperature dependence of the homogenous linewidth.

The last two decades have seen the advent of many laser spectroscopies which can overcome some aspects of the inhomogeneous broadening. The basic principles behind two of the most successful techniques are discussed in the following two chapters.

2. FLUORESCENCE LINE NARROWING

Figure 5 depicts the basic principle of fluorescence line narrowing (FLN). FLN is alternatively called luminescence line narrowing or phosphorescence line narrowing. These terms may be more appropriate depending on the nature of the observed emission. In FLN a subset of chromophores is excited by using a single-frequency (or narrowband) laser. The subset is isoenergetic in the selected transition energy. However, depending on the correlation of energy splittings, the selected subset may be made up from very different sites. As has been discussed above, FLN is basically *energy selective* but not a site selective technique, but due to high correlation of energy levels in crystals it may also be the latter.

Subsequent to the excitation, the fluorescence from the excited subset can be observed either non-resonantly or resonantly to the laser frequency. In the latter case a gating technique has to be applied to discriminate between the resonant luminescence and the laser light. For long-lived excited states (>1 μs) this can be achieved by mechanical choppers but electro- or acousto optic

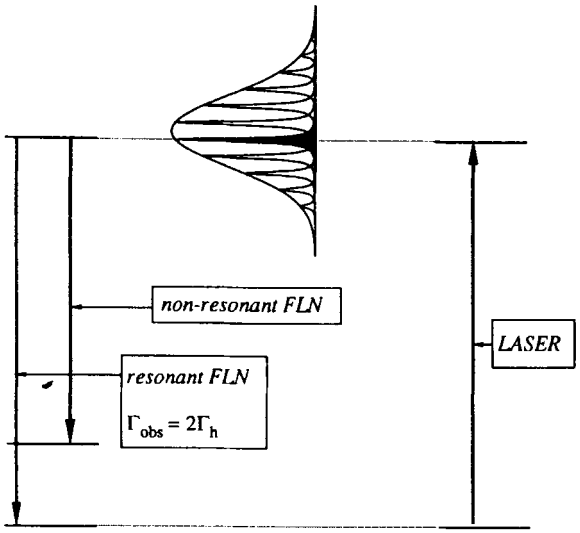

FIGURE 5 Fluorescence Line Narrowing (FLN) in a typical system.

devices have to be applied for faster gating.[14] However, it is easier to achieve high rejection ratios with a mechanical device.

In a system typified in Fig. 5 the observed linewidth in the resonant experiment is given by twice the homogeneous linewidth. This is because FLN is a two photon process. One photon is used to excite a particular subset, and the second photon is then observed in emission.

The lifetime and correlation of the third level is usually determining the linewidth of the non-resonant transition.

In Fig. 6 we show the main components of a typical FLN experiment. The exciting single-frequency laser is passed through the same light chopper as the observed emission but with a phase difference of 180° to avoid laser light reaching the photomultiplier tube. There are practical advantages to replacing the Fabry–Pérot étalon by a monochromator when a resolution of about 0.5 cm^{-1} is adequate (e.g., at high temperatures) as the interferometer always suffers from overlapping orders. The preferred arrangement would couple the output of a monochromator into the étalon. However, the light throughput would often not be adequate.

The finesse of the Fabry–Pérot interferometer often limits the

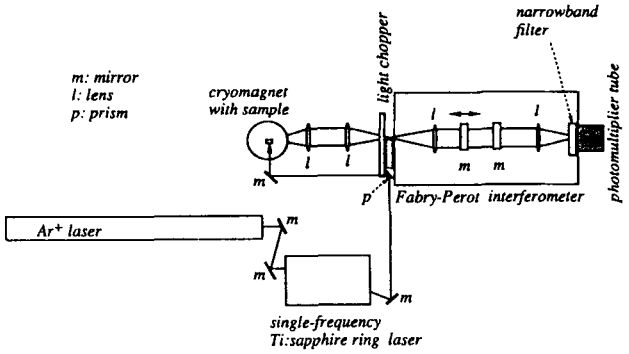

FIGURE 6 Instrumentation for resonant FLN experiments.

resolution in resonantly narrowed FLN spectra, e.g., resolutions below 50 MHz are *not* readily achieved.

3. HOLE-BURNING SPECTROSCOPY

There are several mechanisms which can lead to hole-burning in optical spectra.

3.1. Transient Spectral Hole-Burning

A possible transient hole-burning experiment in a three level system is illustrated in Fig. 7. A single-frequency laser excites a subset of chromophores to the second excited state $|II\rangle$. This state may relax by a direct or multiphonon process with the rate $k_{nr}(II)$ to level $|I\rangle$. When this latter level has a long lifetime it acts as a bottleneck. A second laser may be scanned across the frequency of the first one and a transient hole can be detected in transmission.

Although the most obvious way to perform this experiment is by using two scanning single-frequency lasers it is also possible to perform this experiment by using one laser. In this latter case the output is split and one beam is frequency modulated by an acousto-optic modulator. Since the acousto-optic modulation can be performed on a timescale comparable to the lifetime of level $|I\rangle$ the instrumental broadening due to laser frequency jitter is minimal

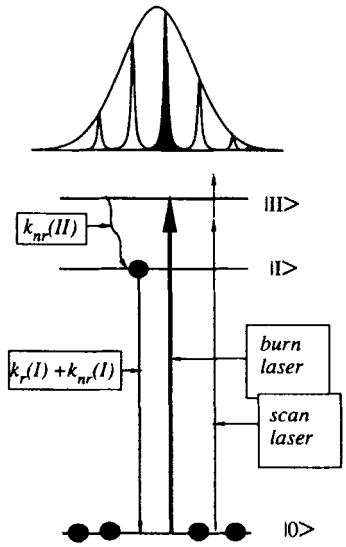

FIGURE 7 Schematic representation of transient hole-burning in a three level system. The long lifetime of |I⟩ leads to a hole observed in the second origin. k_r and k_{nr} denote the radiative and nonradiative relaxation rates, respectively. The burn laser is kept at constant frequency while a second (lower intensity) laser is scanned across the hole.

(only jitter which occurs within the lifetime affects the instrumental linewidth).

Instead of sweeping the laser frequency another approach is to shift the electronic level itself by applying an external electric field (Stark effect). An advantageous situation is presented by a pseudo-Stark splitting. This arises from identical chromophores on inequivalent sites whose orientations of the dipole moments are different.

In a d-d transition the Stark effect is relatively small, but for charge-transfer transitions large Stark shifts can be anticipated. In the experiment an electric field is applied as a sawtooth on a timescale much faster than the lifetime of level |I⟩. If the laser frequency is held constant while the field is rapidly swept, the lineshape of the hole burned at zero field is recovered in transmission.

3.2. Persistent Spectral Hole-Burning

3.2.1. Non-photochemical or photophysical hole-burning. Persistent non-photochemical hole-burning is an utterly ubiquitous phenomenon displayed by molecules and ions embedded in amorphous hosts.[15] Many bulk properties of amorphous hosts can be successfully described by the two-level-system model, TLS, proposed by Phillips[16] and Anderson *et al.*[17] The TLS model describes the non-periodic potential energy surface of a glass as a distribution of double-well potentials. Figure 8 shows how a TLS may be responsible for non-photochemical hole-burning.

After the molecule or the ion is excited it may relax into the second well accompanied by minor rearrangements of the host–

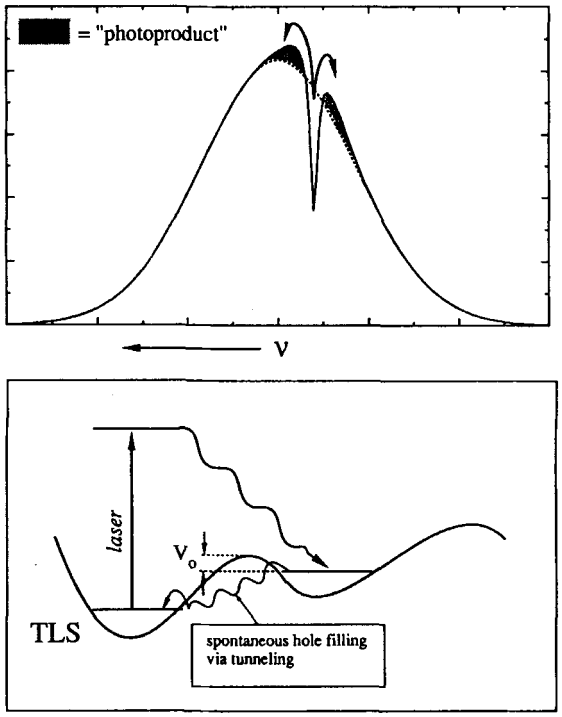

FIGURE 8 Non-photochemical hole-burning and the two level system (TLS) in amorphous hosts.

guest interaction, e.g., hydrogen bonds may be slightly altered. Some of the double wells will have a high activation barrier V_0 and a low tunneling rate from the second well to the first one. Other potentials will either have a low activation barrier and/or relatively fast tunneling rates.

The hole-burning process will produce a distribution of "photoproducts" ranging from rapidly relaxing species to ones that are persistent. Thermally activated hole-filling usually becomes important above 50 K. The changes in the host–guest interaction are minimal in the non-photochemical hole-burning process, and the "photoproduct" will appear as broad (due to poor correlation) anti-holes close to the burned hole (shaded area in Fig. 8).

3.2.2. Photochemical hole-burning. In the photochemical hole-burning process the original chromophore is altered so much that it is a chemically different species. The photoionization of the molecule or ion is the simplest mechanism of photochemical hole-burning, but much more complicated processes like photoinduced ligand exchange can be envisaged. As is depicted in Fig. 9 the photoproduct in the photochemical hole-burning process usually shows an entirely different optical spectrum. In Table I we give a few examples of systems which show photochemical hole-burning.

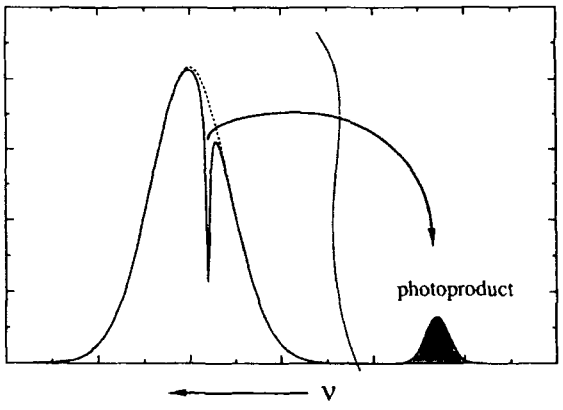

FIGURE 9 Photochemical hole-burning in the solid state.

TABLE I

Photochemical hole-burning. Some systems and proposed mechanisms.

System	Mechanism	Reference
free-base phtalocyanine	proton tautomerization	18
dimethyl-s-tetrazine in crystals and polymers	photodecomposition	19
Co^{2+} in $LiGa_5O_8$	photoionization	20
meso-tetra(p-tolyl)-Zn-tetra-benzo-porphyrin	donor–acceptor electron transfer	21

4. SOME APPLICATIONS

4.1. Non-Resonant and Resonant FLN

A classic example of the power of the non-resonant FLN technique applied to a typical coordination compound is shown in Fig. 10. The luminescence spectrum of $[\{N,N'\text{-bis(2-pyridilmethyl)amine}\}_2 \cdot Cr_2(OH)_2(SO_4)]S_2O_6 \cdot 3H_2O$ could readily be narrowed by exciting into the lowest-excited state, $S^* = 2$.[22] Usually the splitting of the $^4A_2{}^4A_2$ ground state in exchange coupled chromium(III) dimers can be well described by the effective spin Hamiltonian

$$\mathcal{H} = -2J\mathbf{S}_1 \cdot \mathbf{S}_2 - j(\mathbf{S}_1 \cdot \mathbf{S}_2)^2. \tag{9}$$

In the broadband excited luminescence spectrum shown in Fig. 10 the ground state spectrum is not directly observable because the inhomogeneous broadening of the individual transitions is in the same order of magnitude as the actual splittings.

However, in the narrowed spectrum the three non-resonant transitions $S^* = 2 \rightarrow S = 3,2,1$ are fully resolved. From the narrowed spectrum shown in Fig. 10 $J = -7.6$ cm^{-1} and $j = 1.12$ cm^{-1} is deduced. However, both exchange parameters were found to be functions of the excitation wavelength. J ranges from -7.2 to -7.8 cm^{-1} and j from 1.00 to 1.18 cm^{-1} in the inhomogeneous distribution. This variation of the exchange parameters and the large value of j ($\sim$7% of J) suggest that the latter is due to exchange

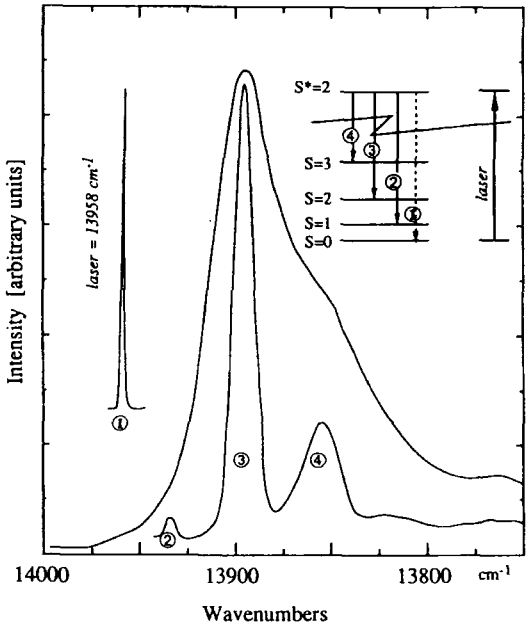

FIGURE 10 Non-resonant FLN in an exchange coupled dimer. [{N,N'-bis(pyridilmethyl)amine}$_2$Cr$_2$(OH)$_2$(SO$_4$)]S$_2$O$_6$·3H$_2$O, at 1.5 K. The insert rationalizes the observed transitions from the lowest excited state to the split $^4A_2{}^4A_2$ ground state.

strictions, i.e., the geometry of the molecular cation changes as a function of the ground state spin level. The relatively large linewidths observed in the narrowed spectrum are partially due to poor correlation but also fast direct relaxation processes within the split ground state are contributing.

It is clear that such detailed information would be difficult if not impossible to extract by the conventional bulk techniques employed in magnetochemistry, e.g., a measurement of the magnetic susceptibility as a function of the temperature.

Using various FLN techniques a controversy about the ^{2}E splitting in crystalline Rh(bpy)$_3$(PF$_6$)$_3$:Cr(III) could be unambiguously resolved.[23] It was also demonstrated that via FLN very accurate g values can be obtained. In Fig. 11 an example of resonant FLN in a magnetic field is shown for this system. The two traces shown were obtained by scanning a plane-parallel Fabry–Pérot interfer-

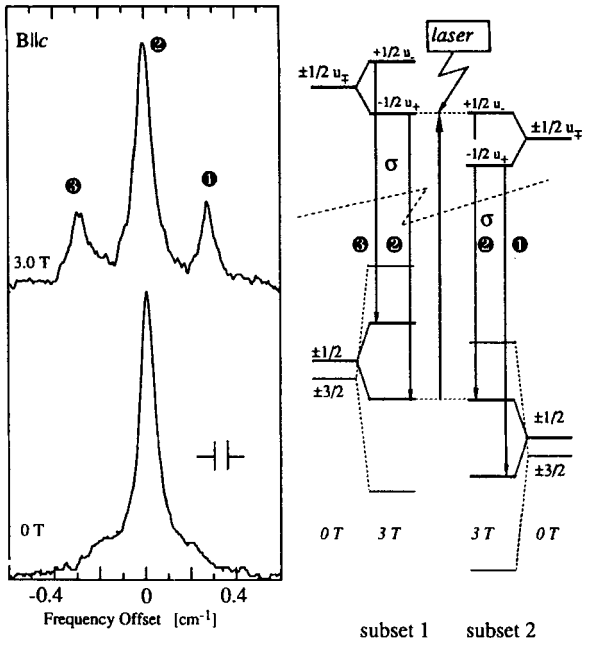

FIGURE 11 Resonant FLN in a d-d transition. The magnetic field is applied perpendicular to the trigonal axis of the $[Cr(bpy)_3]^{3+}$. in $[Rh(bpy)_3](PF_6)_3$ at 4.2 K. A schematic diagram rationalizes the observed three peaks.

ometer. Applying an external field of 3 T, two non-resonant sidelines are observed. The origin of these sidelines is schematically explained in Fig. 11. The precision of g values obtained by narrowing the luminescence spectrum was crucial in being able to unambiguously confirm and improve the results obtained in a former study using conventional spectroscopy.[24] In our work we have also performed the first rigorous linewidth study in a coordination compound. It was found that the homogenous linewidths of R_1 and R_2 were dominated by the direct relaxation process between the split ^2E components in the temperature range of 10 to 100 K.

In Fig. 12 we show an example of resonant FLN in an external magnetic field of the ligand-centered singlet to triplet transition (^3LC) in $[IrCl_2(5,6\text{-dimethyl-phenanthroline})_2]^+$ in a glycerol glass.[25] The inhomogeneous width for this transition was about 650 cm^{-1}. The Zeeman splitting of a spin-only triplet state in a magnetic field

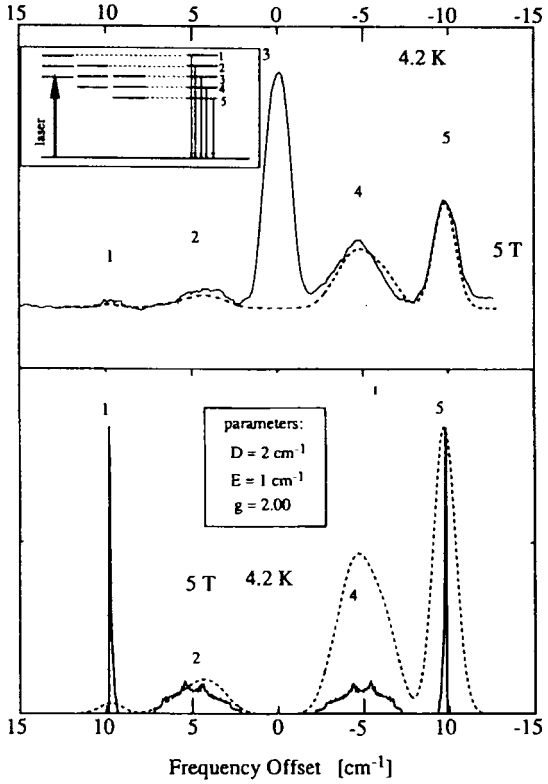

FIGURE 12 Resonant LLN in a ^{3}LC transition. Zeeman effect in the resonantly narrowed luminescence spectrum of $[IrCl_2(5,6\text{-dimethyl-phenanthroline})_2]^+$ in glycerol at 4.2 K. The insert shows a schematic diagram which rationalizes the observed five line pattern for line narrowed singlet–triplet transitions in amorphous hosts. The lower part shows a more detailed calculation of the sideband structure (see text).

of 5 T is about one hundred times smaller than this width and is practically invisible using conventional spectroscopy.

However, the resonantly narrowed FLN shows a well resolved five line pattern. This arises from the three subsets of chromophores that are excited, as is schematically depicted in the upper part of Fig. 12.[26] Of course the schematic explanation shown in Fig. 12 is only a first order approximation, and a better understanding of the lineshapes, widths and intensities of the sidelines

can be gained by a proper calculation. The result of such a calculation is shown in the lower part of Fig. 12. The 3 × 3 matrix of the spin triplet state including the zero field splittings (ZFSs) ($|D| = 2\ cm^{-1}$, $|E| = 1\ cm^{-1}$ assumed) and the elements of the Zeeman interaction in all three directions ($g_x = g_y = g_z = 2.0$) is solved 20,000 times for a randomly oriented (with respect to the direction of the magnetic field) molecule. Assuming the same zero field oscillator strength for the three spin levels, the differences between the eigenvalues are accumulated as a "spectrum", leading to the probability density function shown as the solid line in the lower part of Fig. 12. The dashed curve is the same calculation, but a pseudo-Boltzmann population of the three spin sublevels has been included. The instrumental linewidth of 1.5 cm^{-1} has been convoluted to the calculated sideband spectrum.

As can be seen in the upper part of Fig. 12, the agreement with the experimental spectrum is remarkably good, although for a more precise simulation individual zero field oscillator strengths for the three spin levels and the photoselection factors[27] would have to be taken into account. The large ZFSs observed for $[IrCl_2(5,6\text{-dimethyl-phenanthroline})_2]^+$ are the result of close-lying charge transfer states which strongly perturb the ^{3}LC state.

Resonant FLN in external magnetic fields is an incisive technique in characterizing the nature of luminescent states. Values of the ZFS and their spread can be obtained as well as g values. It is a straightforward method in distinguishing between ^{3}LC and ^{3}MLCT states. The latter may show relatively large ZFSs whereas the ^{3}LC state typically shows splittings in the range of 1 to 10 GHz.

4.2. Hole-Burning Spectroscopy

Figure 13 shows the hole-burning spectrum of the tetragonal complex $[Cr(NH_3)_5Cl]^{2+}$ embedded in ethylene glycol–water (2:1 v/v) at 12 K.[28] A hole is burned with a broadband (30 GHz = 1 cm^{-1}) dye laser into the R_1 line. Notably no sharp hole is detected in the R_2 line. This is due to the fact that the two R lines are poorly correlated in the amorphous matrix, i.e., chromophores with a particular R_1 energy have R_2 energies ranging over the entire inhomogeneous distribution.

We have studied in detail the non-correlation of the R lines of

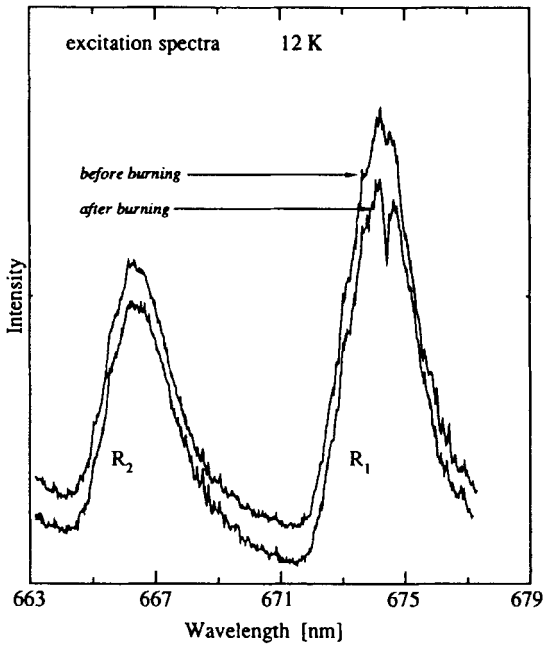

FIGURE 13 Broadband hole-burning in a d-d transition. The spectra of $[Cr(NH_3)_5Cl]^{2+}$ in ethylene glycol water (2:1 v/v) were observed before and after burning in the R_1 line for 30 min by 80 mW.

$[Cr(bpy)_3]^{3+}$ in various amorphous matrices.[29] A remarkable spread of ^2E splittings was found. The intrinsic trigonal symmetry of this molecule is easily broken and low symmetry fields give considerable contributions to the splitting. From a basic perturbation calculation it can be expected that g-values approach the spin-only value rapidly if the (high) trigonal symmetry is perturbed by lower symmetry fields. This phenomenon has been quantified by experiments in which an external magnetic field is used to spread the hole burned into the R_1 line at zero field.

The ground state splitting was found to be poorly correlated in these systems as is illustrated in Fig. 14. After holes were burned into the R_1 line the laser was scanned over 50 GHz and the excitation spectrum was measured. In all spectra two sideholes separated by the ZFS in the $^4A_2$ ground state could be recognized (Fig. 14 shows only the sidehole at higher energy). The sideholes have

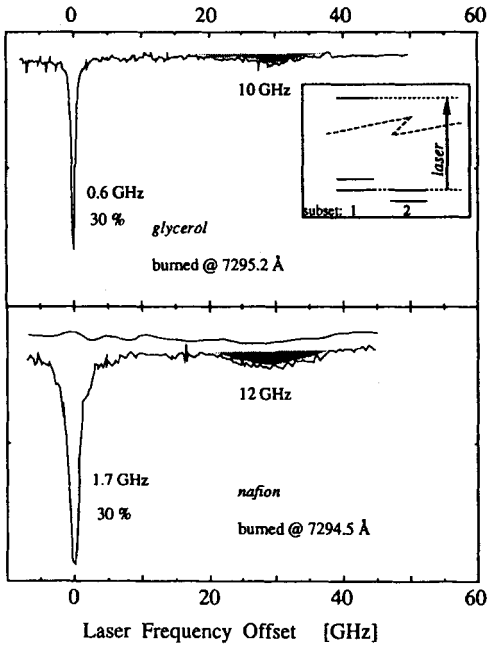

FIGURE 14 High-resolution hole-burning in a d-d transition. The hole is burned in the R_1 line of $[Cr(bpy)_3]^{3+}$ embedded in glycerol and nafion at 1.5 K.

a much bigger linewidth than the resonant hole. This large linewidth is due to the variation of the ground state ZFS from site to site in the amorphous host. Hole-burning is, like FLN, only energy selective and not site selective in amorphous hosts. Thus a large range of sites with varying ZFSs are burned.

In the hole-burning spectrum of $[IrCl_2$(5,6-dimethyl-phenanthroline)$_2]^+$ no sideholes could be detected within the scan width of about 10 GHz.[25] This is consistent with the large ZFS determined in this system by FLN in a magnetic field (see 4.1). The experiment shown in Fig. 15 provided an upper limit for the homogeneous linewidth of the transition to the ^{3}LC state of about 140 MHz in the glycerol host at 1.5 K.

A spectacular example of a transient hole-burning experiment is shown in Fig. 16. The schematic diagram shown in Fig. 7 relates to this particular experiment. However, in this case a single-fre-

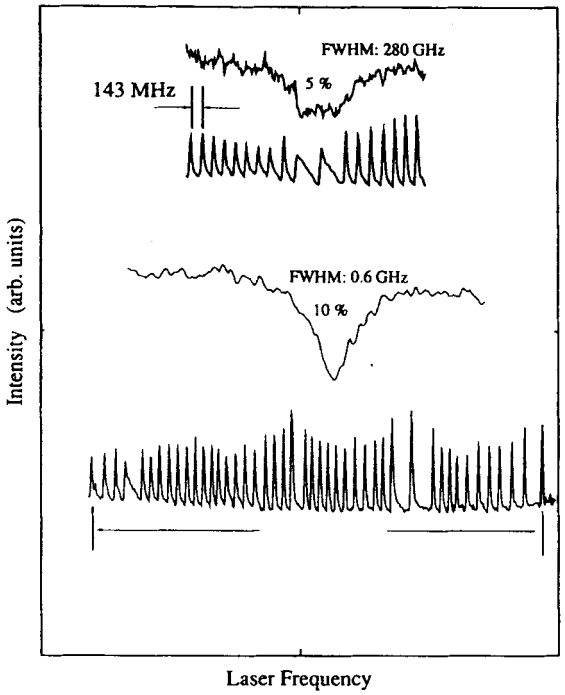

FIGURE 15 Persistent spectral hole-burning of a ^{1}LC transition. $[IrCl_2(5,6\text{-dimethyl-phenanthroline})_2]^+$ in glyerol at 1.5 K. The hole depth and the width are indicated. The holes were read by scanning an Ar^+ laser around 488 nm via the temperature of an intracavity étalon.

quency laser is kept at constant frequency within the inhomogeneously broadened transition to the second excited state (origin II) in $Zn(bpy)_3(ClO_4)_2$:$Ru(bpy)_3^{2+}$, and then the energy of this level is modulated by an external electric field.[30] The pseudo-Stark splitting of origin II provides a very elegant way of recovering the lineshape of the transient hole.

A sawtooth ramp of only ± 3 V/0.5 mm is needed to read out the hole-shape in its entirety! This reflects the large Stark effect determined by the significant change of the electric dipole moment between the ground state and the excited state. This directly establishes the charge-transfer character of the lowest excited states in $[Ru(bpy)_3]^{2+}$. To our knowledge the example given is the first

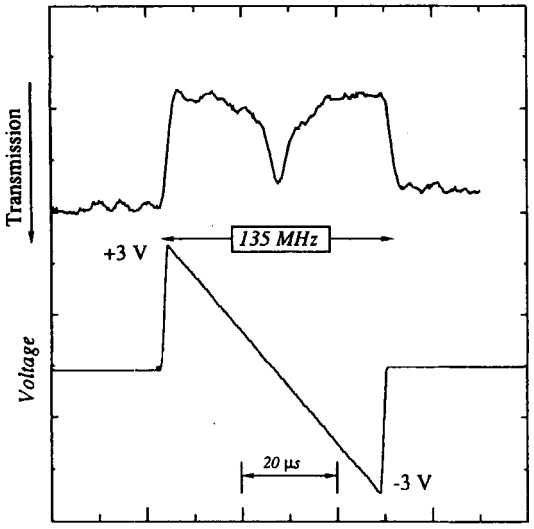

FIGURE 16 Transient spectral hole-burning of a MLCT transition. The hole is burned in the second origin of $[Ru(bpy)_3]^{2+}$ doped in $Zn(bpy)_3(ClO_4)_2$ at 1.5 K. The timescale and the amplitude of the applied sawtooth ramp are indicated.

report of the homogeneous linewidth in a charge-transfer transition. The observed width of ~15 MHz (0.0005 cm^{-1}) is encouragingly small.

Hole-burning and resonant FLN scans establish that there are no ZFS features in the range from 0.1–30 GHz. The features observed in ODMR experiments performed with high microwave powers must have a different source and are not due to a small ZFS of an E state.[31] Nearly degenerate components of an E state would have comparable intensities and would thus easily be detected as side-features in a resonantly narrowed luminescence spectrum.

We have also performed a full rotation study of the resonantly narrowed Zeeman spectrum of the first two electronic origins. An involved rotation pattern is observed consistent with the lowest excited states in $[Ru(bpy)_3]^{2+}$ being localized and non-degenerate. However, relatively fast interligand excitation energy transfer occurs.

5. CONCLUSIONS

The application of advanced laser spectroscopies to coordination compounds is still in its infancy. The examples presented establish these techniques as very promising. Their potential is enormous and many problems in the spectroscopy of this class of materials may eventually be solved by the application of the appropriate laser technique. Whereas a broadband spectrum can in general be rationalized by a whole range of different models, the highly resolved spectrum (MHz range) is far more discriminating. Conventional spectroscopy may be valuable in getting an approximate picture; it is often limited by the inhomogeneous broadening. FLN and spectral hole-burning can be applied to the lowest excited state. However, for higher-lying states the value of these two techniques is diminished as fast relaxation processes lead to relatively large ($1-10\ cm^{-1}$) homogeneous linewidths. In contrast to FLN, hole-burning is not limited to luminescent systems but can be measured in transmission rather than in excitation.

References

1. W. M. Yen and P. M. Selzer (Eds.), *Laser Spectroscopy of Solids, Topics in Applied Physics*, Vol. 49 (Springer-Verlag, Berlin, 1981).
2. R. M. MacFarlane and R. M. Shelby, in *Spectroscopy of Solids Containing Rare Earth Ions*, eds. A. A. Kaplyanskii and R. M. MacFarlane, p. 51 (Elsevier, Lausanne, 1987).
3. S. Völker, Ann. Rev. Phys. Chem. **40**, 499 (1989).
4. W. Moerner (Ed.), *Persistent Spectral Hole-Burning: Science and Applications, Topics in Current Physics*, Vol. 44 (Springer-Verlag, Berlin, 1988).
5. J. Friedrich and D. Haarer, Angew. Chemie Int. Ed. **23**, 113 (1984).
6. R. L. Shoemaker, Ann. Rev. Phys. Chem. **30**, 239 (1979).
7. W. Demtröder, *Laser Spectroscopy, Basic Concepts and Instrumentation* (Springer-Verlag, Berlin, 1982).
8. S. Sugano, Y. Tanabe and H. Kamimura, *Multiplets of Transition Metal Ions* (Academic Press, New York, 1970).
9. G. F. Imbusch and R. Kopelman, in Ref. 1.
10. H. J. Griesser and U. P. Wild, J. Chem. Phys. **73**, 4715 (1980).
11. H. W. H. Lee, C. A. Walsh and M. D. Fayer, J. Chem. Phys. **82**, 3948 (1985).
12. H. Kupka, Mol. Phys. **39**, 849 (1980).
13. K. Kühn, F. Wasgestian and H. Kupka, J. Phys. Chem. **85**, 665 (1981).
14. P. M. Selzer, in Ref. 1.
15. J. M. Hayes, R. Jankowiak and G. J. Small, in Ref. 4.
16. W. A. Phillips, J. Low Temp. Phys. **7**, 351 (1972).

17. P. W. Anderson, B. I. Halperin and C. M. Varma, Phil. Mag. **25**, 1 (1972).
18. A. A. Gorokhovskii, R. Kaarli and L. A. Rebane, JETP Lett. **20**, 216 (1974).
19. H. deVries and D. A. Wiersma, Phys. Rev. Lett. **36**, 91 (1976).
20. R. M. MacFarlane and J. C. Vial, Phys. Rev. B **34**, 1 (1986).
21. T. P. Carter, C. Bräuchle, V. Y. Lee and W. E. Moerner, J. Phys. Chem. **91**, 3998 (1987).
22. H. Riesen and H. U. Güdel, Chem. Phys. Letters **133**, 429 (1987).
23. H. Riesen, J. Luminescence **54**, 71 (1992).
24. A. Hauser, M. Mäder, W. T. Robinson, R. Murugesan and J. Ferguson, Inorg. Chem. **26**, 1331 (1987).
25. H. Riesen, E. Krausz and L. Wallace, J. Phys. Chem. **96**, 3621 (1992).
26. H. Riesen and E. Krausz, Chem. Phys. Letters **172**, 5 (1990).
27. A. C. Albrecht, J. Mol. Spectroscopy **6**, 84 (1961).
28. H. Riesen, N. B. Manson and E. Krausz, J. Luminescence **46**, 345 (1990).
29. H. Riesen and E. Krausz, J. Chem. Phys. **98**, 7902 (1992).
30. H. Riesen and E. Krausz, Chem. Phys. Letters, submitted.
31. (a) S. Yamauchi, Y. Komada and N. Hirota, Chem. Phys. Letters **129**, 197 (1986). (b) H. Yersin, E. Gallhuber, G. Hensler and D. Schweitzer, Chem. Phys. Letters **161**, 315 (1989).
32. H. Riesen and E. Krausz, in preparation for publication.